Supervised Discriminative EEG Brain Source Imaging with Graph Regularization

Feng Liu[1], Rahilsadat Hosseini[1], Jay Rosenberger[1], Shouyi Wang[1], and Jianzhong Su[2]

[1] Department of Industrial, Manufacturing & Systems Engineering,
[2] Department of Mathmatics,
University of Texas at Arlington, Arlington, TX, USA
Email: feng.liu@mavs.uta.edu

Abstract. As Electroencephalography (EEG) is a non-invasive brain imaging technique that records the electric field on the scalp instead of direct measuring activities of brain voxels on the cortex, many approaches were proposed to estimate the activated sources due to its significance in neuroscience research and clinical applications. However, since most part of the brain activity is composed of the spontaneous neural activities or non-task related activations, true task relevant activation sources can be very challenging to be discovered given strong background signals. For decades, the EEG source imaging problem was solved in an unsupervised way without taking into consideration the label information that representing different brain states (e.g. happiness, sadness, and surprise). We showed in this research that by leveraging label information, the task related discriminative sources can be much better retrieved. A novel model for solving EEG inverse problem called Graph Regularized Discriminative Source Imaging (GRDSI) was proposed, which aims to explicitly extract the discriminative sources by implicitly coding the label information into the graph regularization term. The proposed model is capable of estimating the discriminative brain sources under different brain states and encouraging intra-class consistency simultaneously. Simulation results show the effectiveness of our proposed framework in retrieving the discriminative sources.

Keywords: Inverse Problem, Graph Regularization, EEG Source Imaging, Sparse Representation

1 Introduction

Electroencephalography (EEG) is a non-invasive brain imaging technique that records the electric field on the scalp generated by the synchronous activation of neuronal populations. It has been previously estimated that if as few as one in a thousand synapses become activated simultaneously in a region of about 40 square millimeters of cortex, the generated signal can be detected and recorded by EEG electrodes [8][14]. Due to its low cost and exceptional temporal resolution, EEG has become one of the most popular brain imaging tools. Compared to other functional neuroimaging techniques such as functional magnetic resonance imaging (fMRI) and positron emission tomography (PET), EEG is a direct measurement of real-time electrical neural activities, so EEG is more suitable to answer exactly *when* different brain regions are activated and in what processing steps each region is involved [19]. PET and fMRI, by contrast, measure brain activity indirectly through associated metabolic or cerebrovascular changes which are slow and time-delayed [11][14]. To infer the activated brain sources from the recorded EEG data is called *inverse problem*. Precise localization of neuronal firing pattern inside the brain can offer an insightful understanding of how the brain is functioning under certain cognitive and motion tasks. We also argue that source reconstruction or solving the inverse problem is the first and primary step for connectivity analysis of the brain, precise inference of time course of brain sources is required in order to build the brain connectivity network. The latter step is to analyze the brain network using complex networks [6][20][24] characteristics measurement, as we saw a shift in neuroscience community from traditional "segregation" perspective to "integration" perspective [4] where the functional and effective connectivity between different regions of brains are intensively studied [12][18] in recent years.

The pyramidal neurons which are believed to account for most of the EEG signal populate the entire cortical gray matter [2], and outnumber the available sensors by several orders of magnitude, making the inverse problem ill-posed. In order to solve the inverse problem, different priors or assumptions have to be imposed to obtain a unique solution. The most traditionally used priors are based on minimum power, leading to what is known as the minimum norm estimate (MNE) inverse solver [9], or minimum magnitude, termed as minimum current estimate (MCE) [23], leading to a least absolute shrinkage and selection operator (LASSO) formulation. Other assumptions or priors are presented with different inverse algorithms, such as, low-resolution brain electromagnetic tomography (LORETA) [21] and standardized LORETA [22], which enforces spatial smoothness of the source located on neighboring voxels; Bernoulli-Laplace priors, which introduced $\ell_0 + \ell_1$ norm in a Bayesian framework [3]; Mixed Norm Estimates (MxNE), which imposes sparsity over space and smoothness over time using $\ell_{1,2}$-norm regularization [5]; Solution Space Sparse Coding Optimization (3SCO) [26], which is based on particle swarm optimization and an ℓ_0 constraint; graph Fractional-Order Total Variation (gFOTV) [16], which impose sparsity of the spatial fractional derivatives so that it locates source peaks by providing the freedom of choosing smoothness order. As summarized above, numerous algorithms that were based on different source configuration assumptions or prior knowledge were presented to solve the inverse problem. Traditional algorithms solve the EEG inverse problem independently for different brain states without leveraging the label information, that will make it hard to compare the reconstructed sources under different brain states due to its low SNR (Signal-to-Noise Ratio) of the EEG signal. To the best of our knowledge, few researchers come up with a model that can integrate EEG inverse problem with label information (e.g. happiness, sadness, and surprise) to find task related discriminative sources except our previous work [17]. To explicitly extract factual sources and eliminate the spurious ones, we proposed the graph regularized version of discriminative source reconstruction that has the capability of promoting intra-class consistency, and we tested it on synthetic data and illustrated its effectiveness in discovering task related sources. The contributions of this paper are summarized as the following: (1) We propose to use label information to solve the EEG inverse problem in a supervised way. (2) A graph regularized EEG inverse model is presented that can promote intra-class consistency (3) Motivated by the "cross-and-bouquet" model [25], a Voting Orthogonal Matching Pursuit algorithm is proposed to decompose the common sources.

2 The Inverse Problem

Under the quasi-static approximation of Maxwell's equations, the EEG signal measurements X can be described as the following linear function of current sources S:

$$X = LS + E, \tag{1}$$

where $X \in \mathbb{R}^{N_c \times N_t}$ is the EEG data measured at a set of N_c electrodes for N_t time points, $L \in \mathbb{R}^{N_c \times N_d}$ is a wide matrix called lead field matrix that maps the brain source signal to sensors on the scalp, each column of L represents the activation pattern of a particular brain source to the EEG electrodes, $S \in \mathbb{R}^{N_d \times N_t}$ represents the corresponding neural electric field in N_d source locations for N_t time points. $E \in \mathbb{R}^{N_c \times N_t}$ is additive noise. An estimate of S can be found by minimizing the following cost function, which is composed of a data fidelity term and a regularization term:

$$\arg\min_{S} \|X - LS\|_F^2 + \lambda \Theta(S), \tag{2}$$

where $\|\cdot\|_F$ is the Frobenius Norm. The regularization term $\Theta(S)$ can be used to guarantee smooth source configurations temporally or spatially and enforces neurophysiologically plausible solutions or to guarantee sparsity in source solution. For example, to restrict the total number of activated voxels to be less than or equal to k, the constraint $\|s_i\|_0 \leqslant k$ can be used. Even though ℓ_0-norm is the best intuitive formulation to restrict number of activated sources, it's a common practice to use approximated norm such as ℓ_1 to avoid the problem being NP-hard when solving EEG inverse problem. For the ith time point, the ℓ_1 regularized formulation is given below:

$$\langle s_i \rangle = \arg\min_{s_i} \|x_i - Ls_i\|_2^2 + \gamma \|s_i\|_1. \tag{3}$$

Given the EEG recordings at a time point, which is denoted as ith column x_i of X matrix, we want to represent the signal with minimum error by trying to find the best linear representation from activation patterns (atoms) in the over-complete dictionary L [17]. The solution s_i is the sparse coding for the x_i in the dictionary L, the non-zero entries in s_i corresponding to a column in the dictionary matrix L represent the activated regions inside the brain [17]. Solving Problem (3) is relatively a mature technique with many existing algorithms, such as Homotopy, DALM, PDIPA, FISTA, among others listed in Ref.[27].

3 Proposed Framework

3.1 Graph Regularized Discriminative Source Imaging

Due to the fact that EEG signal is non-stationary and typically the SNR is very low, it's important to get consistent inverse solution under the same brain status and eliminate the spurious sources that are usually not consistent within the same class. Inspired by the successful applications of graph regularization in computer vision community [1][7], the proposed model of retrieving task related discriminative source is presented, which is termed as Graph Regularized Discriminative Source Imaging (GRDSI), and comprises the data fidelity term and label guided graph regularization term:

$$\langle S \rangle = \arg\min_{S} \|X - LS\|_F^2 + \gamma \|S\|_{1,1} + \frac{\beta}{2} \sum_{i,j=1}^{N} \|s_i - s_j\|_2^2 M_{ij}, \tag{4}$$

where the first term is the fidelity term, the second term is the cost of sparse coding, $\|\cdot\|_{1,1}$ is the ℓ_1 norm notation for a matrix, equal to the sum of the absolute value of all elements in a matrix. The third term is the graph regularization term that requires all the sparse coder within the same category remains similar pattern while making the sparse representation for different class distinct from each other. The definition of M matrix can be written as:

$$M_{ij} = \begin{cases} 1, & \text{if } (s_i\text{,}s_j) \text{ belong to the same class} \\ 0, & \text{if } (s_i\text{,}s_j) \text{ belong to different classes} \end{cases}$$

The goal of this formulation is to find discriminative sources while maintaining the robustness of in-class reconstructed sources.

Remarks on *design of M matrix*

When (s_i, s_j) belong to the same class, design the value of M_{ij} to be positive will add penalty when the intrinsic geometry (s_i, s_j) is different, thus promoting intra-class consistency of the source and reduce the spurious sources estimated at each time point. The magnitude of M_{ij} can also be adjusted to tailor the relative weight between in-class consistency.

Define D as a diagonal matrix whose entries are column or row sums of the symmetric matrix M, $D_{ii} = \sum_j M_{ij}$, define $G = D - M$, G is called graph Laplacian [1], The third term of Eq.4 can be further derived in the following way:

$$\sum_{i,j=1}^{N} \|s_i - s_j\|_2^2 M_{ij} = \sum_{i,j=1}^{N} ({s_i}^T s_i + {s_j}^T s_j - 2{s_i}^T s_j) M_{ij} = 2tr(S^T G S) \tag{5}$$

As a result, Eq.4 is further derived as:

$$\langle S \rangle = \arg\min_{S} \|X - LS\|_F^2 + \gamma \|S\|_{1,1} + \beta(Tr(S^T G S)) \tag{6}$$

Eq.6 can be efficiently solved using feature-sign search algorithm due to limited space, the readers are encouraged to refer to Ref.[1][15].

3.2 Common Sources Decomposition with Voting Othogonal Matching Pursue(VOMP)

Under the assumption of strong common spontaneous source activation pattern, the contribution of discriminative sources to the EEG recorded data is relatively small, making the solution space for different classes highly correlated and difficult to find discriminative sources. As a result, the convex hull spanned by all the source configuration is limited to a tiny portion of the space [25]. In order to address that, we use the idea of "cross-and-bouquet" model [25] and come up with a useful step that is to decompose of X to find the common sources shared by different classes. Eq.(7) describes the common source decomposition problem.

$$\langle S_c \rangle = \arg\min_{W_c} \|X - LS_c\|_F^2$$
$$s.t.\ \|s_i\|_0 \leqslant T_{max}, \quad i = 1, 2, ...N_d; \quad s_i = s_j, (i = 1, 2, ...N_d, j = 1, 2, ...N_d). \tag{7}$$

The Voting Othogonal Matching Pursue (VOMP) is proposed and described in Algorithm (1). The aim is to recover the common sources across all classes. The core part of VOMP is Othogonal Matching Pursue (OMP) which is an very efficient algorithm. After the decomposition of common source, its contribution to the EEG data X is also removed. The new EEG data after removal of the common source is written as $X_{new} = X - LS_c$. In the following part, we still use X to represent X_{new} when no confusion is caused.

Based on the discussion above, the proposed framework to solve Problem 6 is summarized in Algorithm (2) and illustrated in Fig.1.

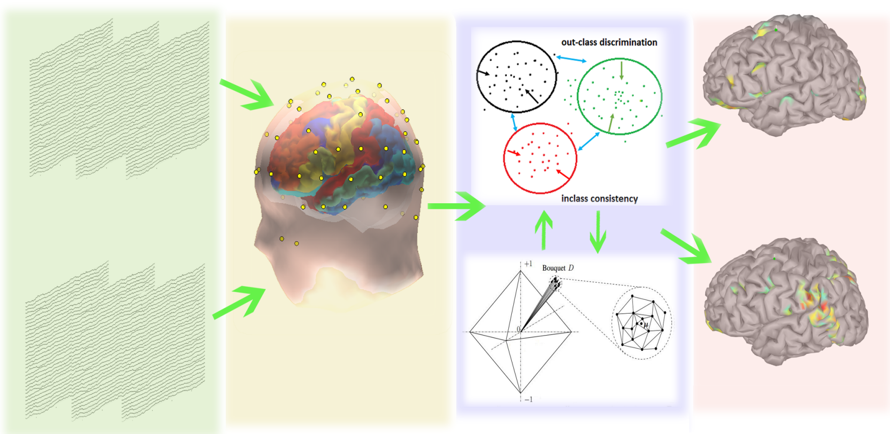

Fig. 1: Procedures of our framework: After gathering labeled EEG recorded data, the brain model is constructed using finite element method (BEM) based on MRI images, the VOMP algorithm is used to decompose the primary common source starting with a high minimum voting percentage, and then solve it using feature-sign search algorithm, the last step is to map discriminative sources to the cortex.

4 Numerical Results

We used a recently developed realistic head model called ICBM-NY or "New York Head" [13]. The dimension of lead field matrix we are using is 108×2004, represent-

Algorithm 1 Decomposition of Non-discriminative Sources with VOMP

INPUT: Lead field matrix L, EEG data X, maximum number of common sources T_{max}, minimum voting acceptance threshold p
OUTPUT: S_c, result of removed common sources X_{new}
Initialization: $T \leftarrow 1$, $\Omega = \emptyset$, $R = X$, $R_{new} = X$, $S' = 0$

while Stopping criteria is not met **do**
  for $i \in 1, ..., N_t$ **do**
    $s_i \leftarrow$ OMP$(L, x_i, 1)$
    $q_i \leftarrow$ nonzero index of s_i
  end for
  $q_{best} \leftarrow$ most frequent q_i
  if $T = T_{max}$ or frequency of $f(q_{best}) < p$ **then**
    break;
  else
    $\Omega \leftarrow \Omega \cup q_{best}$; $L^{'} = (L_{:,i}|i \in \Omega)$; $S^{'} \leftarrow pinv(L')X$; $S^{'} \leftarrow mean(S^{'})$; $R_{new} \leftarrow X - L'S'$
  end if
  for $k \in 1, ..., C$ **do**
    $R^k_{new} = \{R_{new}(i)|i \in \text{class } k\}$;
    $R^k = \{R(i)|i \in \text{class } k\}$
  end for
  if $\left\|R^k_{new}\right\| < \left\|R^k\right\|$ for $k \in 1, ..., C$ **then**
    continue;
  else **break**;
  end if
  $T \leftarrow T + 1$; $R \leftarrow R_{new}$
end while
$X_{new} = R_{new}$; $S_c = S'$
return S_c, X_{new}

ing 108 channels and 2004 voxels. We also assume that source orientation is perpendicular to the cortex surface. In each simulation, noises originate from sensor level and cortex voxel level both contributed to the recorded EEG data. The SNR is calculated as $SNR = 20\log_{10}\frac{\|S\|_2}{\|N\|_2}$.

We show the effectiveness of the graph regularization term in reconstructing the discriminative sources by comparing it with the other eight benchmark algorithms, including ElasticNet, Homotopy, DALM, PDIPA, FISTA, sLORETA, MNE. The former 6 algorithms are compared in image reconstruction applications and can be referred to Ref.[27] for details. We designed the spontaneous common sources with a magnitude of 0.8 with standard deviation to be 0.1 and task related discriminative source with a magnitude of 0.2 with a standard deviation of 0.05 located in different Region Of Interest (ROI)s from the common sources. The ROI we used here are defined in Ref.[10]. We sampled 200 time points for each class and did the experiment 5 times to get the average accuracy of the reconstructed source. For the GRDSI parameter, we set β to be 0.05 and α to be 0.06; The noise matrix is designed to affect the EEG recording together with the true source signal. For each time point, 3 random voxels are corrupted randomly with the average value being 0.2, 0.4, 0.6 and variance being 0.05 based on

Algorithm 2 Proposed framework of solving Problem 6

INPUT: Lead field matrix L, preprocessed EEG signal matrix X, label matrix H
OUTPUT: Discriminative source S_d
Initialization: $T \leftarrow 1$, $\Omega = \emptyset$, $R = X$, $R_{new} = X$, $S' = 0$
while Stoping criteria not met **do**
(1) Using VOMP algorithm for common source decomposition;
(2) Solve the following sparse coding problem for $< s(i) >= \arg\min_{s(i)} L(s_i) + \gamma \|s_i\|_1$ using the feature-sign search algorithm [15] ;
(3) Adjust the voting threshold p;
end while

different SNR design. All computations were conducted on a 64–bit Linux workstation with 3.00 GHz i7-5960x CPU and memory of 64 GB.

The reconstruction performance of the proposed method as well as the benchmark methods based on 150 experiments are summarized in Table 1. All of the values in Table 1, except the Time column (in seconds) represents distance in (mm) from ground true source to the reconstructed source calculated from shortest path along cortex surfaces. PSE represents primary source error, which is the distance of reconstructed primary source to the ground truth primary source. PSE measures the capability of each algorithm to reconstruct the common sources. When the reconstructed location is in a different hemisphere from the ground truth, there is no path connecting those two voxels, so we mark the distance to be 250 mm. EC1 represents error for class 1, which is the distance of the reconstructed discriminative source to the ground truth. EC2 and EC3 are similarly defined.

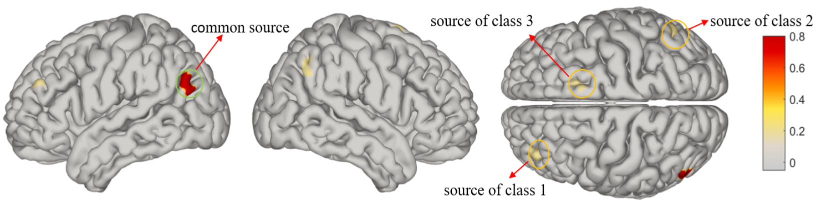

Fig. 2: Ground truth for all 3 classes

To illustrate the effect of the proposed framework, the ground truth of the activated pattern is given in Fig.2, with the reconstructed source by WMN, sLORETA and our method given in Fig.3–5. We can see from Table 1 and the Fig.3–5 that when the SNR is large, all the algorithms performs well in reconstructing primary source, as for the discriminative sources for different classes, our method can achieve almost perfect reconstruction. All other algorithms' performances are also acceptable when SNR is large, except for sLORETA, MNE and ElasticNet. When we increase the noise, all of the algorithms can still achieve high accuracy in finding the primary source. For the discriminative source, our algorithm performs much better. We also validated that, to solve a pure ℓ_1 EEG inverse problem, the Homotopy algorithm performs better in most cases than other algorithms in the EEG inverse problem, which is in line with Ref.[27].

Table 1: Reconstruction Accuracy Summary

	SNR = 10					SNR = 22				
Methods	Time	PSE	EC1	EC2	EC3	Time	PSE	EC1	EC2	EC3
ElasticNet	0.001	43.4	142.3	159.6	159.2	0.001	8.87	172.5	195.0	13.0
Homotopy	0.12	3.43	53.2	42.5	40.8	0.09	0	0.28	0.70	8.00
DALM	0.07	4.59	53.0	43.1	39.6	0.08	0	0.28	1.73	7.98
PDIPA	0.29	3.43	53.4	45.0	40.4	0.26	0	0.28	0.63	7.98
L1LS	3.89	0.69	51.6	67.4	37.1	3.92	0.069	0	0	4.36
FISTA	0.95	**0.63**	61.0	95.2	47.6	0.96	40.1	66.1	73.5	54.5
sLORETA	0.015	10.2	131.7	178.2	142.8	0.02	2.62	194.1	164.2	123.5
MNE	**3e-5**	29.3	131.8	157.7	131.7	**3e-5**	4.30	119.8	136.2	113.5
GRDSI (Proposed)	0.15	1.85	**14.4**	**4.13**	**3.67**	0.10	**0**	**0**	**0**	**2.12**

5 Conclusion

In this paper, we proposed to use label information to retrieve discriminative sources corresponding to different brain status. A graph regularized EEG inverse formulation that implicitly uses the label information was presented that can boost the intra-class consistency and eliminate spurious sources. We bring up the idea of cross-and-bouquet in the inverse problem and present an efficient algorithm to address the high coherence of the reconstructed signals given high background spontaneous source signal. An efficient algorithm called feature-sign search algorithm is used to solve the GRDSI problem. We illustrated the superior of our algorithm in retrieving discriminative sources while traditional algorithms failed given certain level of noises.

References

1. Cai, D., He, X., Han, J., Huang, T.S.: Graph regularized nonnegative matrix factorization for data representation. IEEE Transactions on Pattern Analysis and Machine Intelligence 33(8), 1548–1560 (2011)
2. Castaño-Candamil, S., Höhne, J., Martínez-Vargas, J.D., An, X.W., Castellanos-Domínguez, G., Haufe, S.: Solving the eeg inverse problem based on space–time–frequency structured sparsity constraints. NeuroImage 118, 598–612 (2015)
3. Costa, F., Batatia, H., Chaari, L., Tourneret, J.Y.: Sparse EEG source localization using bernoulli laplacian priors. IEEE Transactions on Biomedical Engineering 62(12), 2888–2898 (2015)
4. Deco, G., Tononi, G., Boly, M., Kringelbach, M.L.: Rethinking segregation and integration: contributions of whole-brain modelling. Nature Reviews Neuroscience 16(7), 430–439 (2015)
5. Gramfort, A., Kowalski, M., Hämäläinen, M.: Mixed-norm estimates for the M/EEG inverse problem using accelerated gradient methods. Physics in medicine and biology 57(7), 1937 (2012)

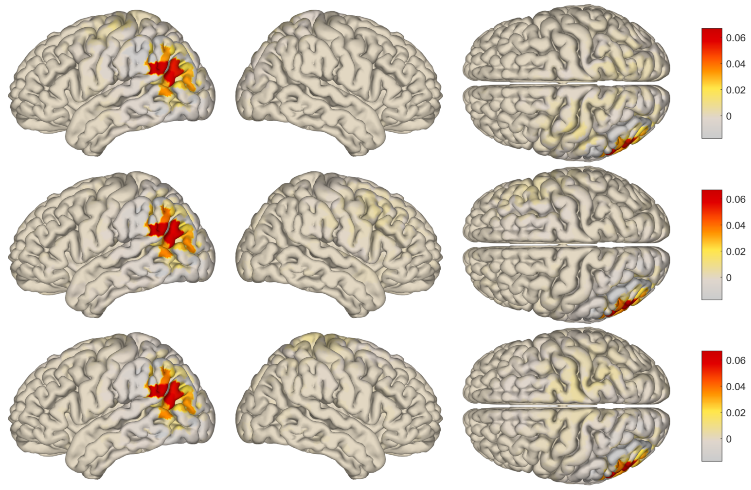

Fig. 3: WMN solution: The above row is the WMN solution for class 1; Class 2 and class 3 is illustrated in the middle and bottom row. The solution WMN gives is not sparse, with too many spurious sources of small magnitude.

6. Guan, Z.H., Liu, F., Li, J., Wang, Y.W.: Chaotification of complex networks with impulsive control. Chaos: An Interdisciplinary Journal of Nonlinear Science 22(2), 023137 (2012)
7. Guo, H., Jiang, Z., Davis, L.S.: Discriminative dictionary learning with pairwise constraints. In: Asian Conference on Computer Vision. pp. 328–342. Springer (2012)
8. Hämäläinen, M., Hari, R., Ilmoniemi, R.J., Knuutila, J., Lounasmaa, O.V.: Magnetoencephalographytheory, instrumentation, and applications to noninvasive studies of the working human brain. Reviews of modern Physics 65(2), 413 (1993)
9. Hämäläinen, M.S., Ilmoniemi, R.J.: Interpreting magnetic fields of the brain: minimum norm estimates. Medical & biological engineering & computing 32(1), 35–42 (1994)
10. Haufe, S., Ewald, A.: A simulation framework for benchmarking EEG-based brain connectivity estimation methodologies. Brain topography pp. 1–18 (2016)
11. Haufe, S., Nikulin, V.V., Ziehe, A., Müller, K.R., Nolte, G.: Combining sparsity and rotational invariance in EEG/MEG source reconstruction. NeuroImage 42(2), 726–738 (2008)
12. Hipp, J.F., Hawellek, D.J., Corbetta, M., Siegel, M., Engel, A.K.: Large-scale cortical correlation structure of spontaneous oscillatory activity. Nature neuroscience 15(6), 884–890 (2012)
13. Huang, Y., Parra, L.C., Haufe, S.: The new york head -a precise standardized volume conductor model for EEG source localization and tes targeting. NeuroImage 140, 150 – 162 (2016), transcranial electric stimulation (tES) and Neuroimaging
14. Lamus, C., Hämäläinen, M.S., Temereanca, S., Brown, E.N., Purdon, P.L.: A spatiotemporal dynamic solution to the meg inverse problem: An empirical bayes approach. arXiv preprint arXiv:1511.05056 (2015)
15. Lee, H., Battle, A., Raina, R., Ng, A.Y.: Efficient sparse coding algorithms. In: Advances in neural information processing systems. pp. 801–808 (2006)
16. Li, Y., Qin, J., Hsin, Y.L., Osher, S., Liu, W.: s-SMOOTH: Sparsity and smoothness enhanced EEG brain tomography. Frontiers in Neuroscience 10, 543 (2016)

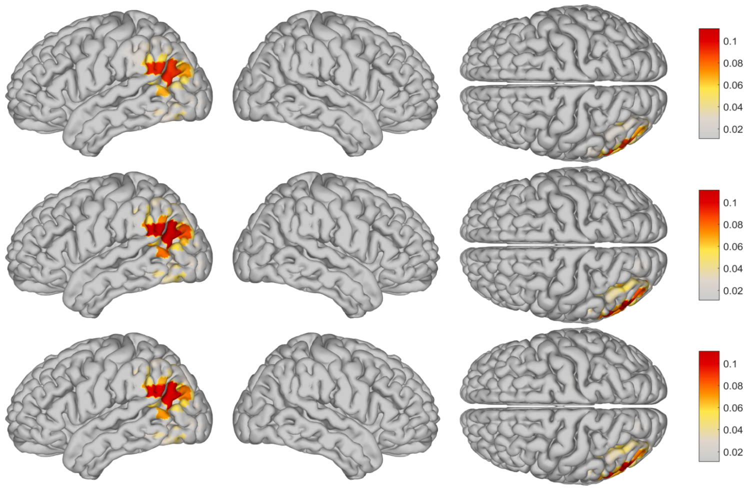

Fig. 4: sLORETA inverse solution: The above row is the sLORETA solution for class 1; Class 2 and class 3 is illustrated in the middle and bottom row. sLORETA can successfully reconstruct the primary source, however the secondary source is not successfully reconstructed. Compared to the solution of WMN, sLORETA can suppress the numerous spurious sources with small magnitude.

17. Liu, F., Wang, S., Rosenberger, J., Su, J., Liu, H.: A sparse dictionary learning framework to discover discriminative source activations in EEG brain mapping. In: AAAI. pp. 1431–1437 (2017)
18. Liu, F., Xiang, W., Wang, S., Lega, B.: Prediction of seizure spread network via sparse representations of overcomplete dictionaries. In: International Conference on Brain and Health Informatics. pp. 262–273. Springer (2016)
19. Michel, C.M., Murray, M.M., Lantz, G., Gonzalez, S., Spinelli, L., de Peralta, R.G.: EEG source imaging. Clinical neurophysiology 115(10), 2195–2222 (2004)
20. Newman, M.E.: The structure and function of complex networks. SIAM review 45(2), 167–256 (2003)
21. Pascual-Marqui, R.D., Lehmann, D., Koenig, T., Kochi, K., Merlo, M.C., Hell, D., Koukkou, M.: Low resolution brain electromagnetic tomography (LORETA) functional imaging in acute, neuroleptic-naive, first-episode, productive schizophrenia. Psychiatry Research: Neuroimaging 90(3), 169–179 (1999)
22. Pascual-Marqui, R.D., et al.: Standardized low-resolution brain electromagnetic tomography (sloreta): technical details. Methods Find Exp Clin Pharmacol 24(Suppl D), 5–12 (2002)
23. Uutela, K., Hämäläinen, M., Somersalo, E.: Visualization of magnetoencephalographic data using minimum current estimates. NeuroImage 10(2), 173–180 (1999)
24. Watts, D.J., Strogatz, S.H.: Collective dynamics of small-worldnetworks. nature 393(6684), 440–442 (1998)
25. Wright, J., Ma, Y., Mairal, J., Sapiro, G., Huang, T.S., Yan, S.: Sparse representation for computer vision and pattern recognition. Proceedings of the IEEE 98(6), 1031–1044 (2010)
26. Xu, P., Tian, Y., Lei, X., Yao, D.: Neuroelectric source imaging using 3sco: A space coding algorithm based on particle swarm optimization and l 0 norm constraint. NeuroImage 51(1), 183–205 (2010)

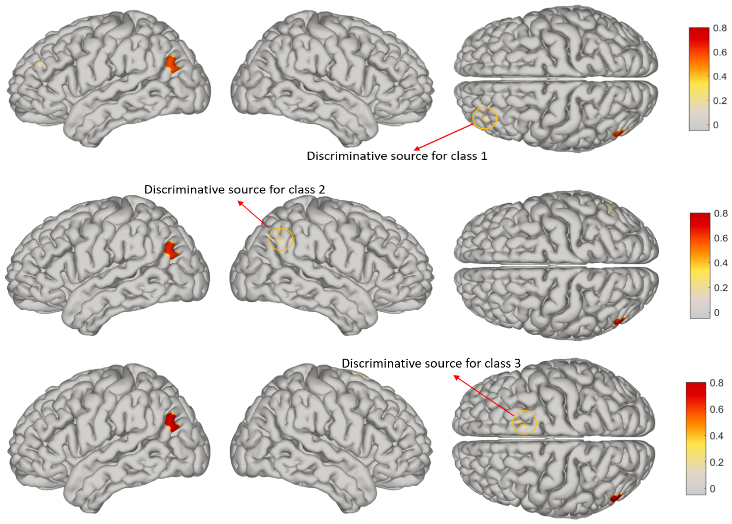

Fig. 5: GRDSI reconstructed source: The reconstruction solutions for 3 classes are given in each row. The discriminative source can be successfully reconstructed compared to other methodologies.

27. Yang, A.Y., Sastry, S.S., Ganesh, A., Ma, Y.: Fast $\ell 1$-minimization algorithms and an application in robust face recognition: A review. In: Image Processing (ICIP), 2010 17th IEEE International Conference on. pp. 1849–1852. IEEE (2010)